Digital Twin Models of Multi-Three-Phase Permanent Magnet Synchronous Motors

Nicola Macrì
Dipartimento Energia 'Galileo Ferraris'
Politecnico di Torino
10129, Turin, Italy
nicola.macri@polito.it

Sandro Rubino
Dipartimento Energia 'Galileo Ferraris'
Politecnico di Torino
10129, Turin, Italy
sandro.rubino@polito.it

Simone Ferrari
Dipartimento Energia 'Galileo Ferraris'
Politecnico di Torino
10129, Turin, Italy
simone.ferrari@polito.it

Gianmario Pellegrino
Dipartimento Energia 'Galileo Ferraris'
Politecnico di Torino
10129, Turin, Italy
gianmario.pellegrino@polito.it

Radu Bojoi
Dipartimento Energia 'Galileo Ferraris'
Politecnico di Torino
10129, Turin, Italy
radu.bojoi@polito.it

***Abstract*—Multiphase motor drives have undergone significant advancements in recent years, particularly in safety-critical applications like wind energy conversion systems, more electric aircraft, or ship propulsion. Compared to their three-phase counterparts, multiphase machines offer several advantages, including reduced per-phase current, lower torque ripple, and inherent fault tolerance. Attractive topology solutions are multi-three-phase (M3PH) machines since they can exploit standard three-phase power electronics technologies, and the know-how related to the three phase drive solutions. The literature proposes several control approaches to deal with M3PH machines, such as vector space decomposition (VSD), multi-stator (MS), and decoupled multi stator (DMS) with its adaptive variant (A-DMS). However, applying these approaches for accurate machine modeling is still challenging, particularly in faulty conditions, and very few articles investigated their systematic implementation in simulation frameworks. Therefore, this paper presents comprehensive and accurate digital twin (DT) models for M3PH machines, ensuring accurate flux and torque production modelling under all potential operating conditions, including open-three phase fault scenarios. The proposed DT models have been developed and validated through simulations on a quadruple three-phase permanent magnet synchronous motor (PMSM).**

Keywords—Multiphase machine modeling, multiphase electrical drives, modular and fault-tolerant machine models, permanent magnet synchronous motors

I. Introduction

Multi-three-phase (M3PH) motors feature multiple three-phase winding sets operated in parallel, resulting in usefulness for safety-critical applications thanks to their modularity and robust fault tolerant design [2] [21]. The machine stator consists of independent three-phase windings with isolated neutral points, each fed by a dedicated three-phase inverter unit, as shown in Fig. 1. This way, the consolidated three-phase technologies can be used [13], [8], significantly reducing costs and design time. Moreover, in the case of a fault, the faulted three-phase winding set is turned off using circuit breakers, stopping the PWM, or actively forced into short-circuit [10], allowing a straightforward post-fault drive configuration.

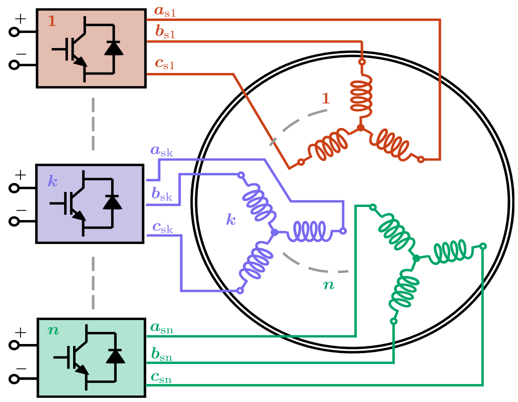

Fig. 1. View of a generic M3PH drive with n three-phase units.

Literature provides different control approaches for M3PH machines (VSD, MS, DMS, A-DMS) [1], [3], each presenting specific pros and cons. However, although these control approaches are well-known in literature, there is almost a complete lack of comprehensive digital twins able to accurately predict the behavior of M3PH machines in normal and faulty conditions, as well as their implementation in simulation frameworks [4], [14].

These models are crucial for implementing DT simulations of M3PH motor drives, which are pivotal for artificial-intelligent applications performing real-time monitoring, fault detection, predictive maintenance and other tasks. Therefore, this paper proposes novel and accurate DT models of M3PH motors by exploiting the control approaches reported in the literature, i.e., VSD, MS, and A-DMS.

This paper is organized as follows: Section II outlines the key aspects of each of the control approaches considered as base layer for the DT models, then deeply described in Section III. Indeed, this section describes DT models in terms of block diagrams, focusing on the core features of each of them, highlighting pros and cons. The simulation results, performed on a quadruple-three-phase permanent-magnet synchronous motor (PMSM) are depicted in Section IV, while Section V concludes this paper.

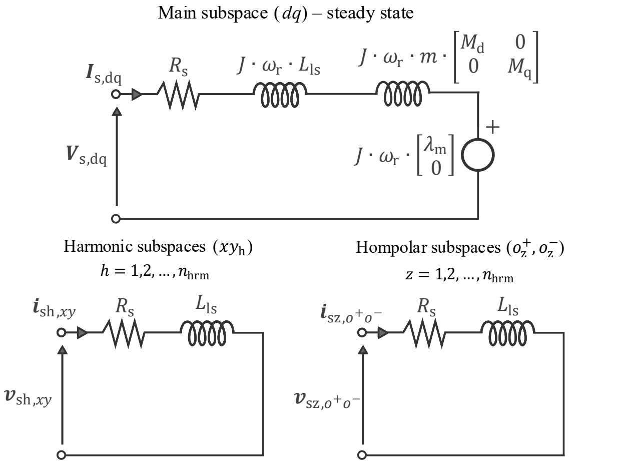

Fig. 2. Steady-state equivalent circuit(s) exploiting VSD modeling on a generic multiphase PMSM. Main *dq* subspace (top), harmonic and homopolar subspaces (bottom).

II. Background

When it comes to modelling and control of a generic multiphase synchronous machine, different methods with unique features can be found in literature. The two widely discussed approaches are Vector Space Decomposition (VSD) and Multi-Stator (MS), also referred to as multiple *d-q* modelling [7]. Indeed, they group the two main transformations applied to the phase variables of a multiphase machine, i.e., a full-order matrix transformation, as the case of VSD, and a set-by-set transformation, as happens when modelling with MS. In essence, the VSD approach models the machine as an equivalent three-phase machine, whereas the MS treats it as multiple three-phase ones. The VSD approach is simple to implement but the result is an *average* machine equivalent model, which doesn't account for flux and torque production of each of the three phase sets, and post-fault configuration is not straightforward. Moreover, this approach cannot deal with irregular stator winding configurations as it is valid only if it is either symmetrical or asymmetrical [15]. On the other hand, the MS approach enhances modularity and post-fault drive configuration is trivial. However, those features come at the cost of heavy cross-coupling between winding sets [12]. The decoupled multi-stator (DMS) control approach, together with its adaptive variant (A-DMS), overcomes this drawback introducing a decoupling transformation, with a similar meaning to the VSD one. The following subsections aim to better understand the core features of the control approaches used for the DT models then described in Section III.

A. Vector Space Decomposition (VSD) Approach

The VSD approach employs a full-order matrix transformation that decomposes the original machine into multiple orthogonal subspaces, thus defining a new equivalent machine model. According to [1], the VSD transformation matrix can be computed for any multiphase machine where the stator windings configuration is well known, either symmetrical or asymmetrical. The algorithm proposed in [1] allows to create a VSD transformation matrix constructed by vertically stacking three submatrices, namely $[T_{\mathrm{nZS}}]$, $[T_{\mathrm{ZS}}]$ and $[ZS]$, as expressed in (1).

$$[T_{\mathrm{VSD}}] = \sigma \begin{bmatrix} [T_{\mathrm{nZS}}] \\ [T_{\mathrm{ZS}}] \\ [ZS] \end{bmatrix} \tag{1}$$

Following the generalized decomposition principles originally introduced by Fortescue in the context of polyphase networks [9], [10], the VSD matrix (1) is arranged in a way that the first components are non-zero-sequence subspaces, followed by zero-sequence subspaces and at the end zero-sequence homopolar subspaces [1]. The constant σ defines whether the matrix is power or amplitude invariant. The submatrices arrangement in (1) allows to understand the meaning of VSD transformation in terms of resulting subspaces: the main $\alpha\beta$ subspace governs electromechanical energy conversion and the equations are the same as an equivalent three-phase machine, while time and spatial harmonics, as well as homopolar zero-sequence patterns, are mapped into *predefined* secondary subspaces, thus exploiting a full *decoupling* between harmonic subspaces. This approach leads to the equivalent circuit depicted in Fig. 2, for fundamental and secondary subspaces. The secondary subspaces are modeled as RL circuits, with stator contributions of resistance and leakage inductance. The transformation is applied directly to the machine variables in phase coordinates. Let $\overline{z}$ denote a column vector representing a generic stator quantity (e.g., voltage, current, or flux linkage). The VSD mapping reads:

$$\overline{z}_{\mathrm{VSD},\alpha\beta} = [T_{\mathrm{VSD}}] \cdot \overline{z}_{\mathrm{ph}} \tag{2}$$

where the left-hand side $\overline{z}_{\mathrm{VSD},\alpha\beta}$ collects the VSD subspaces in stationary coordinates with sequentially ordered components: the first two entries correspond to the $\alpha\beta$ components of the fundamental subspace, followed by the x and y components of each harmonic subspace in order. On the other hand, $\overline{z}_{\mathrm{ph}}$ contains the stator quantity expressed in the original phase domain, whose structure is the following:

$$\overline{z}_{\mathrm{ph}} = \{z_{\mathrm{a}_1}, \dots, z_{\mathrm{a}_\mathrm{n}}, z_{\mathrm{b}_1}, \dots, z_{\mathrm{b}_\mathrm{n}}, z_{\mathrm{c}_1}, \dots, z_{\mathrm{c}_\mathrm{n}}\}^{\mathrm{T}} \tag{3}$$

where *n* is the total number of three-phase units of the machine. The full order transformation provided by VSD enables an equivalent 3-phase machine with the related know-how in terms of modeling, at the cost of handling an *average* model, in which flux and torque contributions of each 3-phase winding set are not highlighted. Indeed, when modeling with VSD, the electromagnetic equations are representative of all stator phases [1], and the overall torque production is expressed as:

$$T = \tfrac{3 \cdot n}{2} \cdot p \cdot (\overline{\lambda}_{\mathrm{s,dq}} \wedge \overline{i}_{\mathrm{s,dq}}) \tag{4}$$

According to (4), modularity is not preserved. If one or more open three-phase faults occur, the drive reconfiguration is not straightforward, since there is need to define a new VSD matrix from scratch. Furthermore, a faulty event is likely to bring the machine into an irregular stator winding configuration, making VSD transformation not feasible anymore.

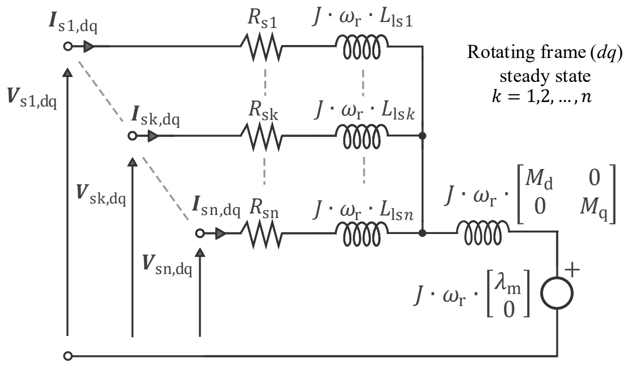

Fig. 3. Steady-state (*dq*) equivalent circuit exploiting MS modeling of a generic multi-three-phase PMSM.

B. Multi-Stator (MS) Approach

The MS approach can be applied only to multi-three-phase machines, since the resultant model is represented by multiple three-phase sets operating in parallel, interacting with each other and the rotor. For each k^{th} three-phase set (k=1÷n), the Clarke transformation is applied [2], thus leading to:

$$\overline{z}_{\mathrm{sk},\alpha\beta} = [C_{\mathrm{k}}]\cdot\overline{z}_{\mathrm{abc,sk}} \tag{5}$$

specifically, a different Clarke transformation is applied for each of the three-phase sets, as expressed in the following:

$$[C_{\mathrm{k}}] = \frac{2}{3}\cdot\begin{bmatrix}\cos\vartheta_{\mathrm{sk}} & \cos\vartheta_{\mathrm{sk}}+2\pi/3 & \cos\vartheta_{\mathrm{sk}}+4\pi/3\\ \sin\vartheta_{\mathrm{sk}} & \sin\vartheta_{\mathrm{sk}}+2\pi/3 & \sin\vartheta_{\mathrm{sk}}+4\pi/3\end{bmatrix} \tag{6}$$

where the matrices C_k are strictly dependent on the characteristic angle of the k^{th} set, i.e. ϑ_{sk}, the displacement between the first phase of the k^{th} set and the α-axis. The latter is conventionally aligned with the first phase of the first set (a_{s1}), so that the matrix C_1 receives ϑ_{s1} = 0°, thus being the same as the Clarke conventionally employed in 3-phase machine modeling (see Fig.4).

The application of the MS leads to a system of n electromagnetic equations, thus highlighting the contributions, in terms of flux and torque, of each of the n three-phase set of the machine. The MS equivalent circuit is depicted in Fig.3.

Indeed, the overall electromagnetic torque is the sum of the contributions of the n sets interacting with the rotor, as expressed:

$$T = \sum_{k=1}^{n} T_k = \frac{3}{2}\cdot p\cdot\sum_{k=1}^{n}\left(\overline{\lambda}_{\mathrm{sk,dq}}\wedge\overline{i}_{\mathrm{sk,dq}}\right) \tag{7}$$

where T_{k} is the torque contribution for the k^{th} set; same considerations for the k^{th} set contributions of flux ($\overline{\lambda}_{\mathrm{sk,dq}}$) and current ($\overline{i}_{\mathrm{sk,dq}}$), while $\wedge$ stands for the operator of outer product.

Modularity is the key feature of the MS modeling approach, which also provides beneficial in the case of one or more open-three phase faults, since it corresponds to zeroing the MS currents of the faulty winding. Analyzing the magnetic model of the machine [2], the following relation applies for each set k:

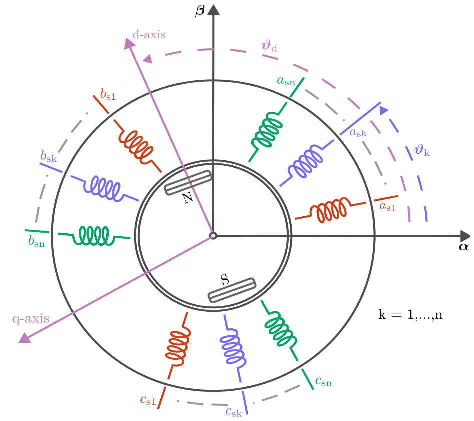

Fig. 4. Generic configuration of a multi-three-phase PMSM: angle displacement between magnetic axes; (*dq*) reference frame.

$$\overline{\lambda}_{\mathrm{sk,dq}} = L_{\mathrm{lsk}}\cdot\overline{i}_{\mathrm{sk,dq}} + \begin{bmatrix}M_{\mathrm{d}} & 0\\ 0 & M_{\mathrm{q}}\end{bmatrix}\cdot\sum_{z=1}^{n}\overline{i}_{\mathrm{sz,dq}} + \begin{bmatrix}\lambda_{\mathrm{m}}\\ 0\end{bmatrix} \tag{8}$$

where L_{lsk} is the k^{th} set leakage inductance, M_{d} and M_{q} the magnetizing inductances, and λ_{m} represents the amplitude of the PM flux linkage, considered as univocal since the sets share the same number of winding turns.

It is noted from (8) that flux linkage of each set is influenced by *dq* currents of the others (z = 1÷n), thus leading to a significant magnetic coupling. Decoupling strategies must be added and implemented to get rid of the coupling terms. The problem can be mitigated considering advanced approaches like the Decoupled Multi-Stator Approach, as described in the next subsection.

C. Decoupled Multi-Stator (DMS) Approach

The DMS approach inherits all the benefits described for the MS, since it is performed starting from MS variables. A decoupling transformation is applied to MS variables to remove the coupling between the three-phase sets. The machine's original space is decomposed into multiple parallel subspaces, similarly to the VSD. The resulting model is again an equivalent three-phase machine, decomposed into a torque-producing subspace, i.e., the common-mode one, and several differential-mode subspaces, whose meaning is to map the unbalances between the three-phase sets, in terms of currents, fluxes and torque. However, according to [1], [2], differential-mode subspaces do not possess the same properties as VSD harmonic subspaces in terms of time-harmonic decoupling [3].

Despite this, DMS equivalent circuits are formally identical to those of VSD modelling, depicted in Fig.2. According to [2], the decoupling transformation matrix can be computed following the structure in (10). It has a power coefficient equal to the number of sets n, thus exploiting its amplitude invariant property. Furthermore, it is a sparse matrix, so its implementation on digital controllers is straightforward. The coefficients w_k and z_k $k=1,\ldots,n-1$ are computed as:

$$w_k = \sqrt{\frac{n\cdot\ n-k}{n-k+1}}\quad,\quad z_k = -\sqrt{\frac{n}{n-k\cdot n-k+1}} \tag{9}$$

$$[T_d] = \frac{1}{n} \cdot \begin{bmatrix} 1 & 1 & 1 & \cdots & 1 & 1 & 1 \\ w_1 & z_1 & z_1 & \cdots & z_1 & z_1 & z_1 \\ 0 & w_2 & z_2 & \cdots & z_2 & z_2 & z_2 \\ 0 & 0 & w_3 & \cdots & z_3 & z_3 & z_3 \\ \vdots & \vdots & \vdots & \ddots & \vdots & \vdots & \vdots \\ 0 & 0 & 0 & \cdots & w_{n-2} & z_{n-2} & z_{n-2} \\ 0 & 0 & 0 & \cdots & 0 & w_{n-1} & z_{n-1} \end{bmatrix} \quad (10)$$

Therefore, a similar equation as (2) can be written:

$$\overline{z}_{\mathrm{DMS,dq}} = [T_{\mathrm{d}}] \cdot \overline{z}_{\mathrm{MS,dq}} \quad (11)$$

where $\overline{z}_{\mathrm{DMS,dq}}$ collects DMS components in terms of common and differential mode, in rotating *dq* coordinates, even though it can be referred to any generic reference frame. On the other hand, $\overline{z}_{\mathrm{MS,dq}}$ represents *dq* components of each of the three-phase sets, once the specific Clarke and rotational transformations are applied. Also, the transformation equation can be written as:

$$\begin{Bmatrix} \overline{z}_{\mathrm{scm,dq}} \\ \overline{z}_{\mathrm{sdm-1,dq}} \\ \vdots \\ \overline{z}_{\mathrm{sdm\ n-1\ ,dq}} \end{Bmatrix} = [T_{\mathrm{d}}]_{\mathrm{n}} \cdot \begin{Bmatrix} \overline{z}_{\mathrm{s1,dq}} \\ \overline{z}_{\mathrm{s2,dq}} \\ \vdots \\ \overline{z}_{\mathrm{sn,dq}} \end{Bmatrix} \quad (12)$$

where the left-hand side contains the resulting DMS components, after the transformation matrix is applied to MS variables. Given this feature, modularity is preserved, since (12) shows that common- and differential-mode vectors are computed as numeric linear combination of MS variables.

However, if one or more open three-phase faults occur, the corresponding MS currents are set to zero, and the decoupling transformation can still be applied to the resulting post-fault MS variables. This means that differential mode currents are different from zero, because the open three-phase fault corresponds to a current unbalance between the winding sets.

Then, as the case of VSD, secondary subspaces (differential- mode ones for DMS) must be properly controlled to keep the machine within balanced operations. Alternatively, if a fault occurs in one or more three-phase units, the DMS transformation can be adapted to consider only the healthy units [2], since there are no constraints on the stator windings configuration. The faulty winding set quantities are neglected, the total number of differential mode subspaces is reduced, and the transformation matrix (10) is recomputed according to the number of active three-phase units. The resulting common and differential modes are automatically adapted, and they are always kept at zero. This approach leads to the so called *Adaptive – Decoupled Multi Stator* (A-DMS), that allows to model a generic multi-three-phase machine into a three-phase equivalent, regardless of the machine operating conditions, whether healthy or faulty. Based on the control approaches described so far, the following section presents the proposed DT models in terms of block schemes, providing an immediate and practical representation that can be explicitly implemented within simulation frameworks to get accurate digital twins of M3PH machines.

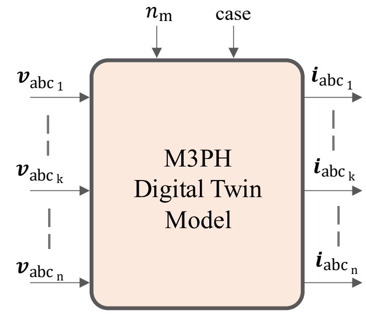

Fig. 5. Generic CCG structure of the proposed DT models.

III. Digital Twin Modeling of M3PH Machines

The need to develop multiple DT models for M3PH machines based on different control approaches arises from the distinct core features required to properly simulate the motor drives. These features include: *i*) modularity, i.e., flux and torque contributions highlighted for each of the three-phase winding set; *ii*) implementation complexity; *iii*) post-fault analysis, i.e., how the simulation model adapts to one or more open three-phase faults; and *iv*) harmonic modelling, i.e., the ability to properly model time and spatial harmonics, as well as torque ripple.

The starting point for each proposed DT model are the set of machine phase variables, in particular, the voltages of each three-phase unit $\boldsymbol{v}_{\mathrm{abc_k}}$ (k = 1,…,n). Also, from the circuital point of view, these DT models correspond to a current-controlled generator (CCG) representation where the state variables are the flux linkages [6]. The generic motor structure, globally valid for all the models, is depicted in Fig. 5, where the inputs are the phase voltages, the motor speed and an external configuration signal (*case*) that defines the machine supply configuration (whether healthy or faulty), so the model can adapt to it in a way that will be discussed further in the paper.

Regardless of the control approach used as the base layer for the DT model, an accurate direct current-to-flux and inverse flux-to-current model must be employed. This enables the following models to also handle highly saturated machines, where these magnetic models can be extremely nonlinear [11].

Furthermore, incorporating the rotor electrical position into these mappings is crucial, since synchronous machines can be significantly influenced by harmonic components of the magnetic field [6], which may lead to distortions in the back-EMF and generate torque ripple [14], even more pronounced in faulty conditions [5]. This dependence, combined with nonlinear saturation and slotting effects [13], leads to angular variations that must be captured to ensure accurate modeling of the machine's electromagnetic response under all operating conditions [12], [16]. According to Fig. 4, if the α-axis is taken as reference, the rotor electrical position coincides with the d-axis.

A. Flux-to-current Model

The current-to-flux model, i.e., $\lambda_{\mathrm{dq}}(I_{\mathrm{d}}, I_{\mathrm{q}}, \vartheta_{\mathrm{d}})$, has been obtained through the finite element analysis (FEA) reported in literature [5] and mapped with SyR-e [18] for healthy and several possible open-set derating conditions [19]. In order to exploit the $\mathrm{dq}\vartheta$ maps formulation, the flux maps are computed over a regular square current domain, with a fine rotor step

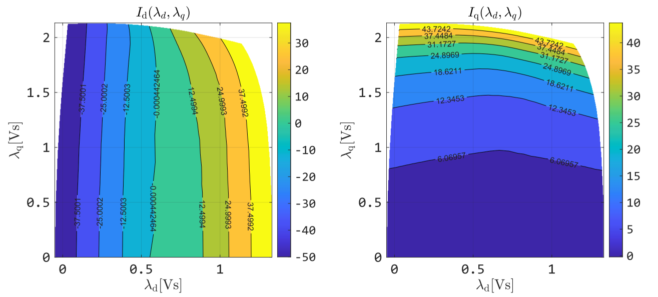

Fig. 6. Inverse unnormalized magnetic model for a fixed value of ϑ_d.

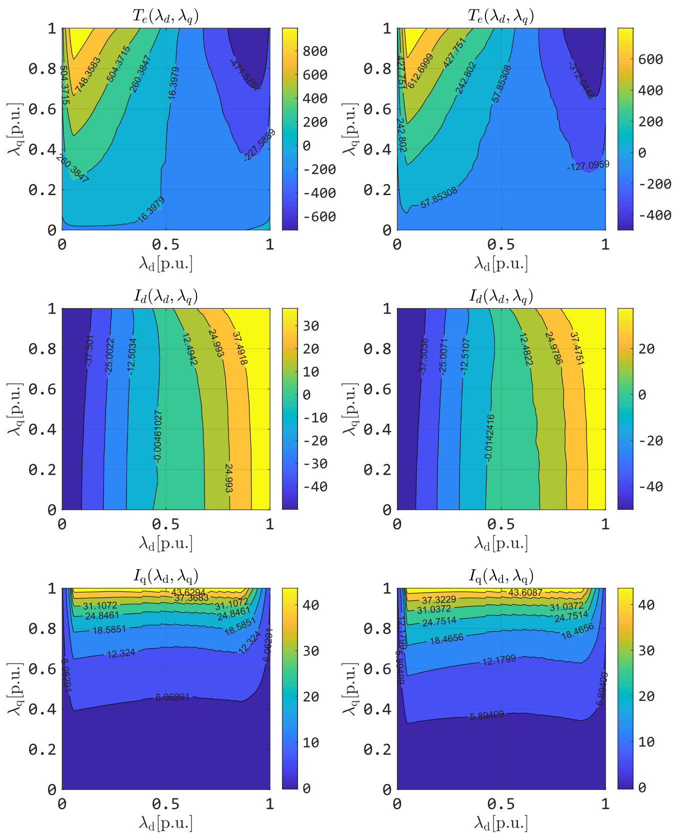

Fig. 7. Inverse normalized magnetic model for a fixed value of ϑ_d, for the healthy configuration (left) and a faulty configuration (right).

condition (rotation of 2 electrical degrees between each simulation). The inverse model is computed from the direct model. Unfortunately, the flux domain in such maps is very irregular (see Fig.6), regardless of the supply configuration. This means that its implementation and interpolation in both simulation environments and digital controllers is nontrivial. A domain regularization strategy must be implemented. Let's assume that, for a given value of the rotor electrical displacement, the flux in d axis is expressed in *per-unit* (p.u.), where 0 stands for its minimum value, 1 for its maximum. On the other hand, flux linkage in q axis is normalized in the same way, but for each value of ϑ_d and λ_d. This way, a square flux domain is obtained (Fig. 7), and the resulting inverse model can be easily interpolated as a look-up table (LUT). According to the above description, reference flux in both axis is computed in corresponding pu values following (13).

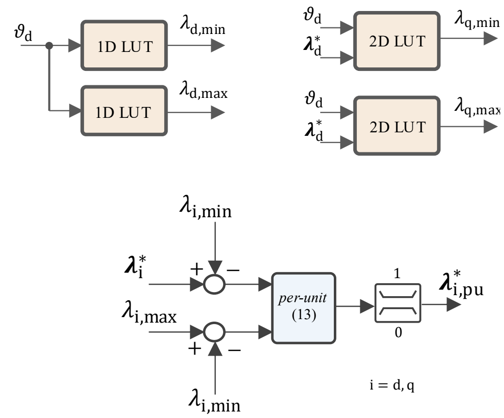

Fig. 8. Maximum and minimum flux profiles interpoolation (top); per-unit flux computation in the generic i axis ($i = d,q$) (bottom).

$$\lambda_{i,pu} = \frac{\lambda_i^* - \lambda_{i,min}}{\lambda_{i,max} - \lambda_{i,min}} \tag{13}$$

Minimum and maximum values of the flux linkage, in d and q axis are obtained by interpolation of LUTs, whose block diagram is depicted in Fig. 8 (top).

The flux inputs of the normalized inverse maps are retrieved from (13), as shown in Fig. 8 (bottom). Finally, such maps are interpolated using linear 3D interpolation methods, whose implementation is straightforward [11]. The results, exploited for both healthy and faulty configuration, are depicted in Fig. 7.

The following subsections will finally describe the proposed DT models, making clearer the importance of the inverse magnetic model.

B. VSD-based DT Model

The first proposed DT model builds upon the VSD approach, previously introduced in Section II-A. The complete implementation of this model for a generic M3PH is illustrated in Fig. 9, which shows the entire simulation structure based on this method.

Starting with the supply voltages of each three-phase set, the corresponding flux linkages in phase coordinates are dynamically computed, exploiting the voltage equation:

$$v_{abc_k} = R_s \cdot i_{abc_k} + \frac{d}{dt}\lambda_{abc_k} \tag{14}$$

it is noted that (14) is valid under all operating conditions, including open-three-phase faults. The VSD transformation is thus applied to flux linkages of each three-phase set, according to (2) and (3). At this point, the resulting subspaces can be treated separately, thus exploiting the full decoupling feature among VSD subspaces. The currents related to the fundamental subspace are obtained from the normalized inverse magnetic model in dq reference frame, once the per-unit reference values of flux are computed following Fig. 8. Furthermore, thanks to the *case* signal externally imposed, the model will automatically adapt the fundamental subspace to a possible fault scenario, thus interpolating different inverse models according to the supply configuration. Same considerations apply for the electromagnetic torque. The currents of the multiple harmonic subspaces are instead modeled to include the

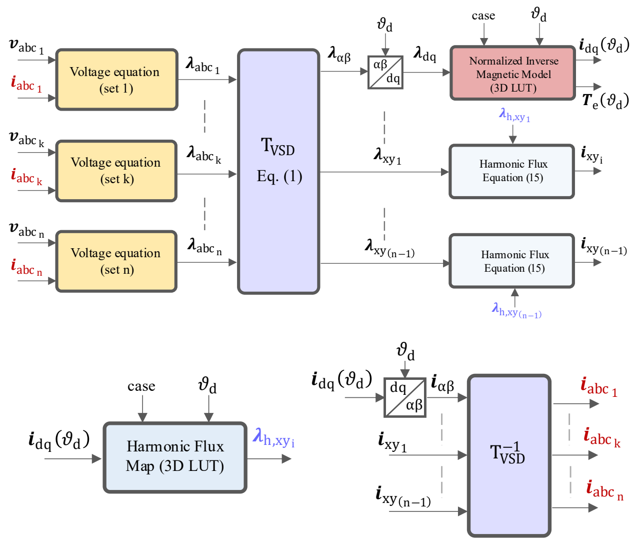

Fig. 9. Proposed DT model based on VSD control approach.

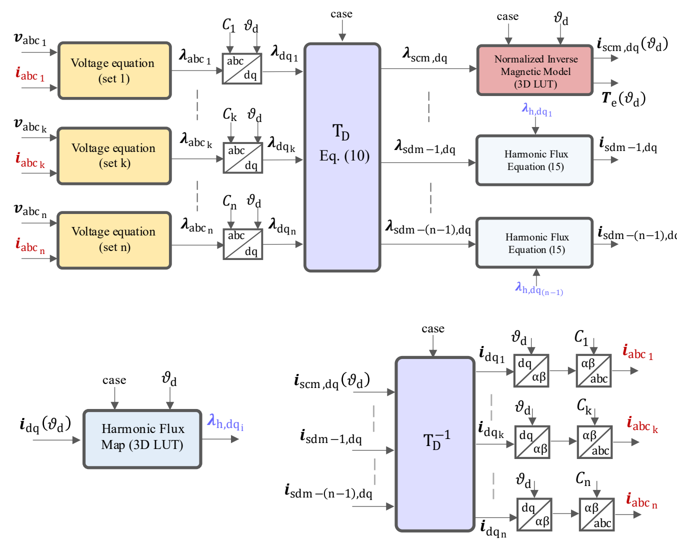

Fig. 10. Proposed DT model based on ADMS control approach.

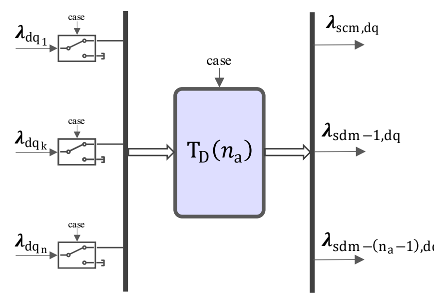

Fig. 11. Scheme of the adaptive decoupling transformation.

harmonic flux contribution imposed by the PM field, as described by:

$$\lambda_{\mathrm{h,xy_i}} = \lambda_{\mathrm{xy_i}} - L_{\mathrm{ls}} \cdot i_{\mathrm{xy_i}} \qquad \mathrm{i} = 1, \dots, \ \mathrm{n}-1 \tag{15}$$

where, for each harmonic subspace, a constant leakage inductance is considered.

Starting from (15), a look-up table has been developed to include this flux contribution for every machine operating point, including faulty scenarios.

This LUT is interpolated from the feedback of *dq* currents in the fundamental subspace, and the rotor electrical displacement.

Finally, the machine currents in phase coordinates, for each of the three-phase sets, are obtained from the inverse VSD transformation. Such currents are fed back to the voltage equations (14). Although the model depicted in Fig. 9 is easy to implement, it does not emphasize the flux and torque contributions of each individual three-phase winding set.

Besides, it requires appropriate acting on the supply voltages to model one or more open three-phase faults since the VSD transformation matrix cannot be adapted to these scenarios.

C. DMS and ADMS-Based DT Model

The DMS-based DT model follows a similar structure of the VSD-based one, with the main difference lying in the transformation domain. Specifically, the decoupling transformation (10) is applied to *dq* fluxes of each three-phase set after Clarke and rotational transformations, thus exploiting common- and differential mode fluxes. Furthermore, the harmonic flux map follows (15), but it is computed considering the DMS approach, thus obtaining such fluxes in differential-mode subspaces. Nevertheless, compared to VSD-based model, modularity is preserved, according to (12). This property allows to model possible open-three-phase faults by setting to zero the related MS currents, without acting on the supply voltages.

However, in those cases, additional control modules must be added to actively control the secondary subspaces. Conversely, as explained in Section II-C, the DMS approach allows changing on the fly the decoupling transformation, thus adapting it to the postfault configuration of the stator windings. The resulting ADMS model, depicted in Fig. 10, shares the same structure as the DMS-based one, with the key difference being that the decoupling transformation block receives the *case* signal as input. According to it, the fluxes of the faulty winding set are simply neglected, and the decoupling transformation is recomputed only considering the total number of active winding sets n_a, as schematically shown in Fig. 11. As in the DMS model, common-mode currents are retrieved from the inverse magnetic model, while differential-mode currents are computed via (15).

Again, harmonic flux maps are computed following the dedicated A-DMS approach. Finally, given the inverse decoupling block that follows the same scheme as Fig. 11, output currents in phase coordinates are computed being the feedback of voltage equations. According to the A-DMS approach, output currents of the faulty windings are inherently set to zero. Finally, it is worth noting that the DMS DT model can be implemented using the same structural framework shown in Fig. 10, provided the case signal input is removed and the harmonic flux mapping is adapted accordingly.

IV. Simulation Results

The motor under test is a quadruple three-phase PM-assisted synchronous motor with an asymmetric winding configuration (15 degrees of phase displacement between adjacent three phase sets). The machine's primary data is collected into Table I. Imposing a reference operating point in *dq* frame, sinusoidal voltage supply is provided for each of the four three-phase sets.

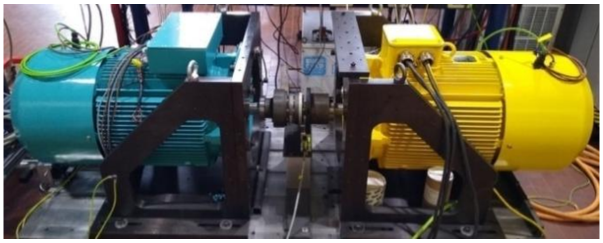

Fig. 12. View of the M3PH prototype (left, blue motor), torque transducer (middle), and driving machine (right, yellow motor).

TABLE I. MACHINE PRIMARY DATA

Machine Data	
Phase number	12 (4×3-phase)
Pole number	2
Rated power	60 kW
Rated speed	1000 r/min
Stator resistance	260.8 mΩ
Stator leakage inductance	7 mH

The resulting phase current and torque waveforms are shown in Figs. 13 and 14, respectively. These two simulations were performed without and with the inclusion of the permanent magnet (PM) harmonic flux contribution, as described in (15). This comparison highlights the waveform distortions introduced by harmonic effects.

In particular, Fig. 13 shows nearly sinusoidal phase currents, with a small ripple introduced by the effect of the rotor electrical displacement. Conversely, Fig. 14 reveals noticeable distortion in the output phase currents, caused by the presence of the PM harmonic flux contribution. The output torque waveform includes ripple components, as it is computed from dqϑ LUTs (see Section III.A), which inherently captures the rotor-position-dependent variations in electromagnetic torque [12]. It is noted that all the proposed DT models can simulate such behaviors, as the results obtained with different approaches lead to overlapped waveforms. Same considerations can be made in the case of one or more open three-phase faults, despite the differences in how each approach models the system, as discussed in Section IV. Furthermore, Figs. 15 and 16 illustrate the models' behavior under open three-phase fault conditions affecting two out of the four winding sets. Specifically, Fig. 15 refers to the case where sets 3 and 4 are faulted, while Fig. 16 corresponds to the scenario in which sets 2 and 4 are lost.

According to the finite element analysis reported in the literature [5], the fault scenario deeply influences torque ripple.

This is mainly due to the different shapes of the airgap flux density and the additional harmonic generated by uneven machine supply [19]. Proof of this statement is shown by output torque waveforms [21]. For both simulations, the average torque is the same but losing sets 2 and 4 leads to a slightly reduced torque ripple, with respect to losing sets 3 and 4. Although the VSD, DMS, and ADMS digital twin models yield to identical results in terms of output quantities such as phase currents and electromagnetic torque, the ADMS approach offers significant advantages from a modeling and control perspective [17]. Unlike VSD and DMS, which require active control of harmonic or differential-mode subspaces to maintain balanced operations,

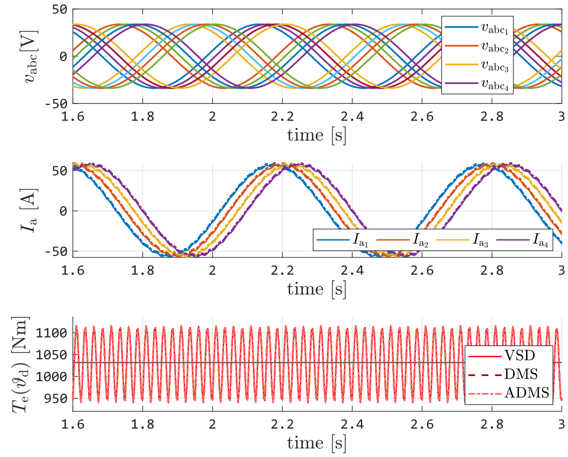

Fig. 13. Simulation for the healthy configuration without including PM harmonic flux contibution: supply voltages, output phase *a* currents, output torque. VSD (solid line), DMS (dotted line), ADMS (dash-dot line).

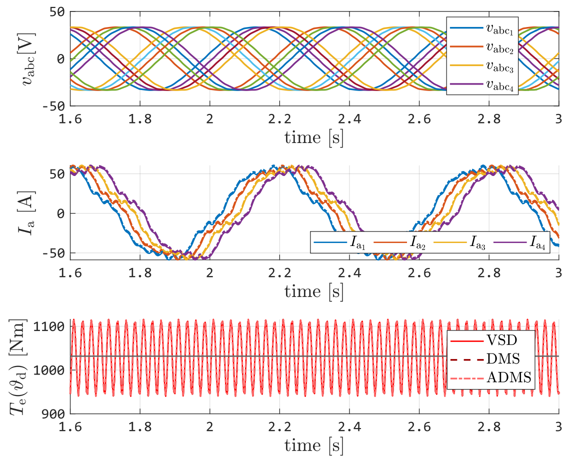

Fig. 14. Simulation for the healthy configuration including PM harmonic flux contibution: supply voltages, output phase *a* currents, output torque. VSD (solid line), DMS (dotted line), ADMS (dash-dot line).

especially under fault conditions, the ADMS formulation inherently suppresses these subspaces, that are always at zero.

This structural property simplifies the control architecture, reduces the need for additional regulators, and enhances modularity, making ADMS particularly suited for scalable and fault-tolerant implementations of multi-three-phase drives.

V. CONCLUSION

This paper presented a comprehensive framework for DT modeling of M3PH permanent magnet synchronous motors, based on established control approaches, like VSD, DMS and ADMS. Each DT model has been systematically developed and tested to simulate the motor's behavior under various operating conditions, including open-three-phase fault scenarios. Such models incorporate detailed flux-to-current and current-to-flux mappings derived from finite element analysis, ensuring accurate representation of magnetic saturation and rotor position effects. The simulation results confirm that all the proposed DT models can accurately replicate the machine's electromagnetic behavior in terms of phase currents and torque, both in healthy and faulty states, including the effects of PM harmonic flux components. While VSD and DMS-based models offer viable simulation options, they come with limitations in modularity –

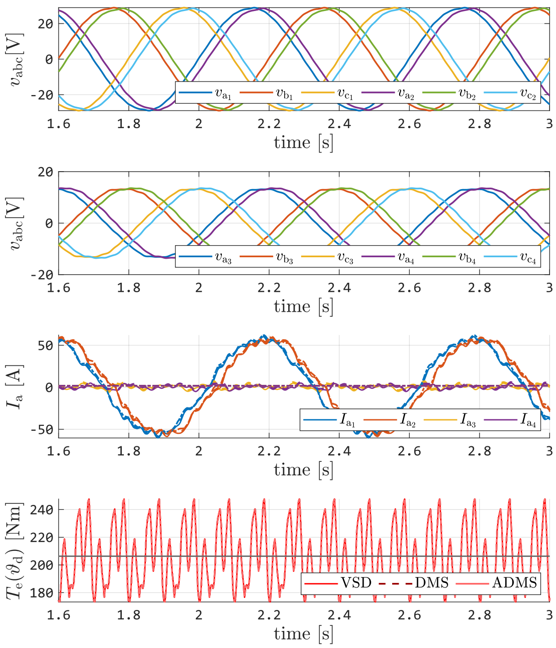

Fig. 15. Simulation with open three-phase fault on units 3 and 4: supply voltages, output phase *a* currents, output torque. VSD (solid line), DMS (dotted line), ADMS (dash-dot line).

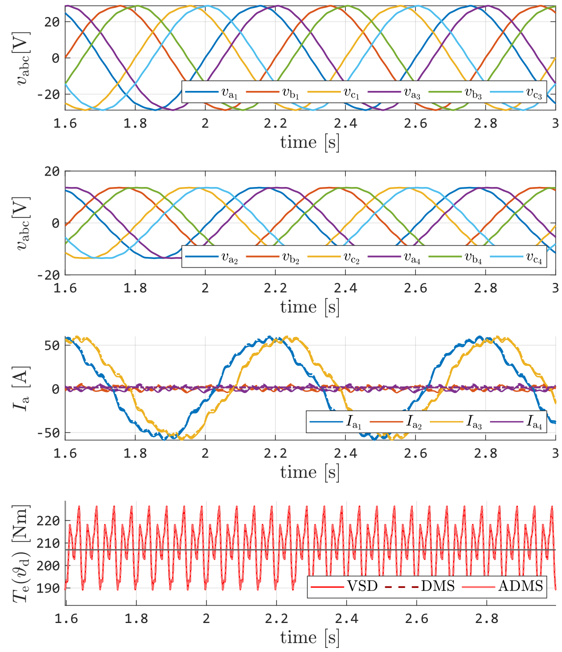

Fig. 16. Simulation with open three-phase fault on units 2 and 4: supply voltages, output phase *a* currents, output torque. VSD (solid line), DMS (dotted line), ADMS (dash-dot line).

as the case of VSD – post-fault adaptability and control complexity. The ADMS approach, on the other hand, overcomes these limitations by preserving modularity, automatically adapting to faulty configurations without structural changes, and inherently suppressing secondary subspaces. These features significantly reduce control complexity and enhance scalability.

Therefore, among the proposed modeling approaches, the ADMS-based DT model emerges as the most versatile and robust solution, offering an optimal trade-off between modeling accuracy, modularity, and implementation simplicity for scalable and fault-tolerant M3PH motor drive systems.

REFERENCES

[1] I. Zoric, M. Jones, and E. Levi, “Vector Space Decomposition Algorithm for Asymmetrical Multiphase Machines”. *19th International Symposium Power Electronics Ee2017*, October 19-21,2017, Novi Sad, Serbia.

[2] S. Rubino *et al.*, “Fault-Tolerant Torque Controller Based on Adaptive Decoupled Multi-Stator Modeling for Multi-Three-Phase Induction Motor Drives,” *IEEE Trans. Ind. Appl.*, vol. 57, no. 6, Dec. 2022.

[3] I. Zoric, M. Jones and E. Levi, “Arbitrary Power Sharing Among Three-Phae Winding Sets in Multiphase Machines”, *IEEE Trans. Ind. Appl.*, vol. 65, no. 2, Feb. 2018.

[4] A. G. Yepes *et al.*, "Current harmonic compensation in symmetrical multiphase machines by resonant controllers in synchronous reference frames - Part 1: Extension to any phase number," *IEEE Annual Conf. of the Industrial Electronics Society IECON*, Vienna, Austia, pp. 5155 - 5160, 2013.

[5] S. Ferrari et al., "Performance Derating of Multi-Three-Phase PM-Assisted Synchronous Reluctance Motors in Open-Three-Phase Fault Condition," *2024 IEEE ECCE*, Phoenix, AZ, USA, 2024, pp. 5573-5580.

[6] A. Bojoi, S. Ferrari, P. Pescetto and G. Pellegrino, “Advanced Circuital Model for e-Drive Simulation, Including Harmonic Effects and Fault Scenarios”, *PCIM Europe* 2023, 09 – 11 May 2023, pp. 1580-1589.

[7] M. J. Duran and F. Barrero, “Recent advances in the design, modeling, and control of multiphase machines—Part II,” *IEEE Trans. Ind. Electron.*, vol. 63, no. 1, pp. 459–468, Jan. 2016.

[8] F. Meinguet et al., "Fault-tolerant operation of an open-end winding five-phase PMSM drive with inverter faults," *IECON 2013*, Vienna, Austria, 2013, pp. 5191-5196

[9] Y. Zhao and T. A. Lipo, “Space vector PWM control of dual three-phase induction machine using vector space decomposition,” *IEEE Trans. Ind. Appl.*, vol. 31, no. 5, pp. 1100–1109, Sep. 1995.

[10] C. L. Fortescue, “Method of Symmetrical Co-ordinates Applied to the Solution of Polyphase Networks,” *34th Annual Convention of the American Institute of Electrical Engineers*, June 1918.

[11] M. Ferrari, N. Bianchi, and E. Fornasiero, “Rotor saturation impact in synchronous reluctance and pm assisted reluctance motors,” in *2013 IEEE Energy Conversion Congress and Exposition*, 2013, pp. 1235– 1242.

[12] M. Zabaleta, E. Levi, and M. Jones, “Modelling approaches for triple three-phase permanent magnet machines,” in *Proc. XXII Int. Conf. Elect. Mach.*, 2016, pp.466–472.

[13] L. De Camillis *et al.*, "Optimizing current control performance in double winding asynchronous motors in large power inverter drives," *IEEE Trans. on Power Electronics*, vol. 16, no. 5, pp. 676 - 685, 20.

[14] M. Slunjski *et al.*, “Symmetrical/asymmetrical winding reconfiguration in multiphase machines,” *IEEE Access*, vol. 8, pp. 12835–12844, 2020.

[15] G. K. Singh, K. Nam, and S. K. Lim, “A simple indirect field-oriented control scheme for multiphase induction machine,” *IEEE Trans. Ind. Electron.*, vol. 52, no. 4, pp. 1177–1184, Aug. 2005.

[16] Y. Hu, Z. Q. Zhu, and K. Liu, “Current control for dual three-phase permanent magnet synchronous motors accounting for current unbalance and harmonics,” *IEEE J. Emerg. Sel. Topics Power Electron.*, vol. 2, no. 2, pp. 272–284, Jun. 2014.

[17] X. Wang *et al.*, "Diagnosis-Free Self-Healing Scheme for Open-Circuit Faults in Dual Three-Phase PMSM Drives," in *IEEE Transactions on Power Electronics*, vol. 35, no. 11, pp. 12053-12071, Nov. 2020.

[18] S. Ferrari, G. Pellegrino et al. "SyR-e: Synchronous Reluctance - evolution" Available at https://github.com/SyR-e/syre_public/tree/v25.1

[19] S. Ferrari, S. Rubino and G. Pellegrino, "Effect of Rotor Type on Open-Set Derating Operations of Multi-Three-Phase Synchronous Machines," *2025 IEEE (IEMDC)*, Houston, TX, USA, 2025, pp. 795-800

[20] K. Nounou *et al.*, “Emulation of an electric naval propulsion system based on a multiphase machine under healthy and faulty operating conditions,” *IEEE Transactions on Vehicular Technology*, vol. 67, no. 8, pp. 6895–6905, 2018.

[21] A. Akay and P. Lefley, “Research on torque ripple under healthy and open-circuit fault-tolerant conditions in a PM multiphase machine,” *CES Transactions on Electrical Machines and Systems*, vol. 4, no. 4, pp. 349–359, Dec. 2020.